Vibrationally Resolved Photoelectron Spectroscopy of BO^- and BO_2^-: A Joint Experimental and Theoretical Study

Hua-Jin Zhai,[†,‡] Lei-Ming Wang,[†,‡] Si-Dian Li,[*,§] and Lai-Sheng Wang[*,†,‡]

Department of Physics, Washington State University, 2710 University Drive, Richland, Washington 99354, Chemical Sciences Division, Pacific Northwest National Laboratory, MS K8-88, P.O. Box 999, Richland, Washington 99352, and Department of Chemistry and Institute of Materials Sciences, Xinzhou Teachers' University, Xinzhou 034000, Shanxi, People's Republic of China

Received: October 11, 2006; In Final Form: October 31, 2006

We report a photoelectron spectroscopy and computational study of two simple boron oxide species: BO^- and BO_2^-. Vibrationally resolved photoelectron spectra are obtained at several photon energies (355, 266, 193, and 157 nm) for the ^{10}B isotopomers, $^{10}BO^-$ and $^{10}BO_2^-$. In the spectra of $^{10}BO^-$, we observe transitions to the $^2\Sigma^+$ ground state and the $^2\Pi$ excited state of ^{10}BO at an excitation energy of 2.96 eV. The electron affinity of ^{10}BO is measured to be 2.510 ± 0.015 eV. The vibrational frequencies of the ground states of $^{10}BO^-$ and ^{10}BO and the $^2\Pi$ excited state are measured to be 1725 ± 40, 1935 ± 30, and 1320 ± 40 cm^{-1}, respectively. For $^{10}BO_2^-$, we observe transitions to the $^2\Pi_g$ ground state and two excited states of $^{10}BO_2$, $^2\Pi_u$, and $^2\Sigma_u^+$, at excitation energies of 2.26 and 3.04 eV, respectively. The electron affinity of $^{10}BO_2$ is measured to be 4.46 ± 0.03 eV and the symmetrical stretching vibrational frequency of the $^2\Pi_u$ excited state of $^{10}BO_2$ is measured to be 980 ± 30 cm^{-1}. Both density functional and ab initio calculations are performed to elucidate the electronic structure and chemical bonding of the two boron oxide molecules. Comparisons with the isoelectronic AlO^- and AlO_2^- species and the closely related molecules CO, N_2, CN^-, and CO_2 are also discussed.

1. Introduction

Boron monoxide (BO) and dioxide (BO_2) are the simplest boron oxide species and have attracted persistent interest over the past four decades, primarily due to their roles in the combustion of boron and boranes.[1] The $^2\Sigma^+$ ground state of the BO radical has been well-characterized by using high-resolution spectroscopy[2−6] as well as high-level calculations.[7,8] The $^{11}B^{16}O$ molecule possesses a bond length of 1.2049 Å, a bond energy of 8.34 eV, and a vibrational frequency of 1885.69 cm^{-1} in its $^2\Sigma^+$ ground state, while its first excited state $^2\Pi$ lies about 2.96 eV above the ground state with a bond length of 1.3533 Å and a vibrational frequency of 1260.70 cm^{-1}.[2] BO_2 is a prototypical linear Renner−Teller molecule,[9] and has been an intriguing species particularly for vibrational spectroscopic studies. Following the first absorption[3] and matrix spectral work[10] in the early 1960s, a large body of spectroscopic[11] and computational studies[8,12,13] on BO_2 has appeared in the literature. Among the electronic states characterized are the $^2\Pi_g$ ground state and the $^2\Pi_u$, $^2\Sigma_u^+$, and $^2\Sigma_g^+$ excited states.[3,6,8,9−13]

However, the electronic properties of the BO^- and BO_2^- anions have received rather limited experimental attention. The only experimental report thus far is the photoelectron spectroscopy (PES) of $^{11}BO^-$ at 351 nm.[14] The electron affinity (EA) of BO was elusive for decades. An earlier experimental EA value was obtained from the equilibrium data to be 2.84 eV in 1971,[15] and a lower limit of 2.48 eV was assigned slightly earlier in 1970.[16] Numerous theoretical studies also generated inconsistent EA values, ranging from 2.17 to 2.79 eV.[7,8] In 1997, the theoretical group of Schaefer[17] and the experimental group of Lineberger[14] concurrently reported more accurate experimental (2.508 ± 0.008 eV) and theoretical (2.57 eV) EA values for BO. These new values provided the benchmark for further theoretical studies.[18] The situation for BO_2^- is worse and there is still no consensus about the EA of BO_2. The available experimental EA values of BO_2 derived from the equilibrium data range from 3.28 to 4.33 eV.[15,16,19] On the other hand, theoretical predictions for the EA of BO_2 also span a large range from 3.9 to 4.65 eV.[8,13,20] Clearly, more accurate determination for the EA of BO_2 is called for.

Boron possesses unique and diverse chemistries due to its electron deficiency.[21] In the past few years, we have been interested in elucidating the novel structural and electronic properties and chemical bonding in elemental boron clusters[22,23] and boron alloy clusters[24−26] using PES in combination with high-level theoretical calculations. The current work represents a continuation of our interest in boron chemistry. In this contribution, we report a detailed PES study of $^{10}BO^-$ and $^{10}BO_2^-$. Vibrationally resolved PES data were obtained at several photon energies (355, 266, 193, and 157 nm). The EA values of ^{10}BO and $^{10}BO_2$ were measured to be 2.510 ± 0.015 and 4.46 ± 0.03 eV, respectively. The obtained vibrational frequencies and excitation energies are compared with previous high-resolution spectroscopic data. Theoretical calculations were performed at B3LYP and CCSD(T) levels for both BO^- and BO_2^- and their neutrals.

2. Experimental and Computational Methods

2.1. Photoelectron Spectroscopy. The experiment was carried out by using a magnetic-bottle-type PES apparatus

* Address correspondence to this author. E-mails-: ls.wang@pnl.gov (L.S.W.); lisidian@yahoo.com (S.D.L.).
† Washington State University.
‡ Chemical Sciences Division, Pacific Northwest National Laboratory.
§ Xinzhou Teachers' University.

10.1021/jp0666939 CCC: $37.00
Published on Web 01/25/2007

equipped with a laser vaporization supersonic cluster source, details of which have been described previously.[27] Briefly, the $^{10}BO^-$ and $^{10}BO_2^-$ anions were produced by laser vaporization of a pure disk target made of enriched ^{10}B isotope (99.75%) in the presence of a pure helium carrier gas. The oxide species $^{10}BO^-$ and $^{10}BO_2^-$ with sufficient abundance were produced along with pure B_n^- clusters due to the residual oxygen from the target surface. Clusters from the laser vaporization source were analyzed by using a time-of-flight mass spectrometer. The $^{10}BO^-$ and $^{10}BO_2^-$ species were each mass-selected and decelerated before being photodetached. Four detachment photon energies were used in the current study: 355 (3.496 eV), 266 (4.661 eV), and 193 nm (6.424 eV) for $^{10}BO^-$, and 193 and 157 nm (7.866 eV) for $^{10}BO_2^-$. Photoelectrons were collected at nearly 100% efficiency by the magnetic bottle and analyzed in a 3.5 m long electron flight tube. The photoelectron spectra were calibrated by using the known spectrum of Rh^- and Au^-, and the resolution of the apparatus was $\Delta Ek/Ek \approx 2.5\%$, that is, ~25 meV for 1 eV electrons.

2.2. Computational Methods. DFT structural optimizations and frequency analyses were performed by using the hybrid B3LYP procedure[28] with the augmented Dunning's all-electron basis set (aug-cc-pVTZ)[29] implemented in Gaussian 03.[30] Excitation energies of the neutrals were calculated with the time-dependent DFT (TD-DFT) method[31] at the ground state structures of the anions. Coupled cluster calculations (CCSD(T))[32] were further performed to evaluate the adiabatic and vertical detachment energies (ADE's and VDE's) at the DFT geometries.

3. Experimental Results

3.1. BO^-. The PES spectra of $^{10}BO^-$ were recorded at three photon energies (355, 266, and 193 nm), as shown in Figure 1. The 355 nm spectrum (Figure 1a) exhibits a well-resolved short vibrational progression for the ground state (X). The 0−0 transition at 2.510 ± 0.015 eV defines the VDE as well as the ADE for $^{10}BO^-$, which also represents the EA of the ^{10}BO neutral. The ground state vibrational frequency of ^{10}BO is measured to be 1935 ± 30 cm^{-1} from the observed vibrational progression. The hot band transition (labeled as "HB" in Figure 1a) at 2.30 eV yields the anion ground state vibrational frequency as 1725 ± 40 cm^{-1}. The 266 nm spectrum (Figure 1b) did not reveal additional electronic transitions. The first excited state of ^{10}BO could only be observed in the 193 nm spectrum (Figure 1c). In contrast to the ground state transition, a long vibrational progression (A) with a vibrational frequency of 1320 ± 40 cm^{-1} was observed for the transition to the first excited state of ^{10}BO. The 0−0 transition defines an ADE of 5.47 ± 0.02 eV for band A, whereas the 1←0 transition at 5.63 ± 0.02 eV represents the VDE. The ADE difference between bands X and A defines an excitation energy of 2.96 eV for the first excited state of ^{10}BO. The hot band transitions for band A yielded the same vibrational frequency for the $^{10}BO^-$ anion as band X. The obtained spectroscopic constants are collected in Table 1.

3.2. BO_2^-. Due to its high electron binding energies, only 193 and 157 nm spectra were recorded for $^{10}BO_2^-$, as shown in Figure 2. The 193 nm spectrum shows only a single band X with a VDE of 4.46 ± 0.03 eV. Since no vibrational structures were observed, suggesting little geometry change between the ground states of $^{10}BO_2^-$ and $^{10}BO_2$, the single peak also defines the ADE or the EA of $^{10}BO_2$ as 4.46 ± 0.03 eV. At 157 nm, two more bands were revealed (Figure 2b). Band A at 6.72 ± 0.02 eV ADE (or VDE) exhibited a well-resolved vibrational progression with a spacing of 980 ± 30 cm^{-1}. Band B at 7.50 ± 0.02 eV showed one single vibrational peak. Bands A and B represent the first and second excited states of $^{10}BO_2$ with excitation energies of 2.26 and 3.04 eV, respectively. The obtained spectroscopic constants are also summarized in Table 1.

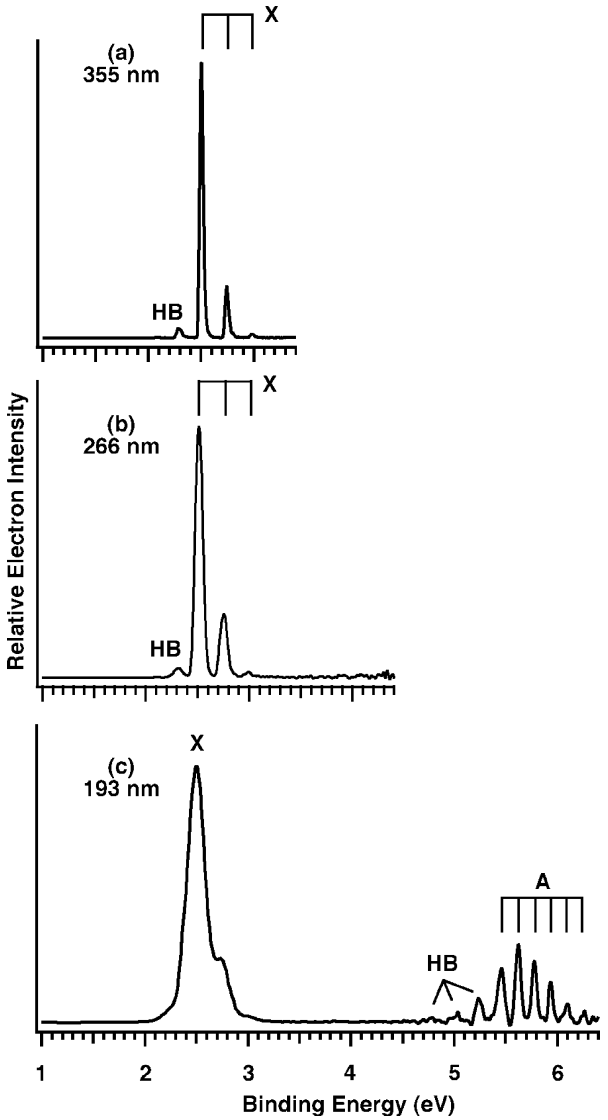

Figure 1. Photoelectron spectra of BO^- at (a) 355 (3.496 eV), (b) 266 (4.661 eV), and (c) 193 nm (6.424 eV). HB represents hot band transitions.

4. Theoretical Results

4.1. BO^-. At the B3LYP level, the ground states of ^{10}BO ($^2\Sigma^+$) and $^{10}BO^-$ ($^1\Sigma^+$) were calculated to have bond lengths of 1.203 and 1.234 Å, bond energies of 8.41 and 9.32 eV, and vibrational frequencies of 1913 and 1739 cm^{-1}, respectively. The calculated ADE and VDE for BO^- are 2.588 and 2.627 eV, respectively. The slight energy difference between the ADE and VDE originates from the 0.031 Å bond length change between BO^- and BO. The VDE for the first excited state of BO was predicted to be 5.900 eV at the TD-B3LYP level. Single point CCSD(T) calculations were further done at the B3LYP geometries, yielding ADE (2.484 eV) and VDE (2.497 eV) slightly lower than those at the B3LYP level. All calculated spectroscopic data are given in Table 2 to be compared with the experimental results (Table 1).

TABLE 1: Observed Adiabatic and Vertical Detachment Energies, Term Values, and Vibrational Frequencies from the Photoelectron Spectra of $^{10}BO^-$ and $^{10}BO_2^-$

species	feature	ADE (eV)	VDE (eV)	term value (eV)[a]	vib freq (cm^{-1})[b,c]
$^{10}BO^-$	X	2.510 ± 0.015[d]	2.510 ± 0.015	0.00	1935 ± 30[e]
	A	5.47 ± 0.02	5.63 ± 0.02	2.96[f]	1320 ± 40
$^{10}BO_2^-$	X	4.46 ± 0.03[g]	4.46 ± 0.03	0.00	
	A	6.72 ± 0.02	6.72 ± 0.02	2.26[f]	980 ± 30[h]
	B	7.50 ± 0.02	7.50 ± 0.02	3.04[f]	

[a] Defined as the difference of ADE relative to that of the ground state X. [b] The observed vibrational frequencies are for neutral ground and excited states of ^{10}BO and $^{10}BO_2$. [c] Vibrational frequencies of ^{10}BO and $^{10}BO^-$ are obtained from the Franck−Condon factor simulations (see Figure 4). [d] Electron affinity of the ^{10}BO neutral. The electron affinity of ^{11}BO was reported previously as 2.508 ± 0.008 eV (ref 14). [e] Anion ground state vibrational frequency of $^{10}BO^-$ is measured to be 1725 ± 40 cm^{-1} from the observed hot band transitions for both band X and band A (Figure 1). [f] The term values are identical with those from high-resolution spectroscopy of neutral BO (refs 2 and 3) and BO_2 (refs 3 and 9). [g] Electron affinity of the $^{10}BO_2$ neutral. [h] The totally symmetric vibrational frequency.

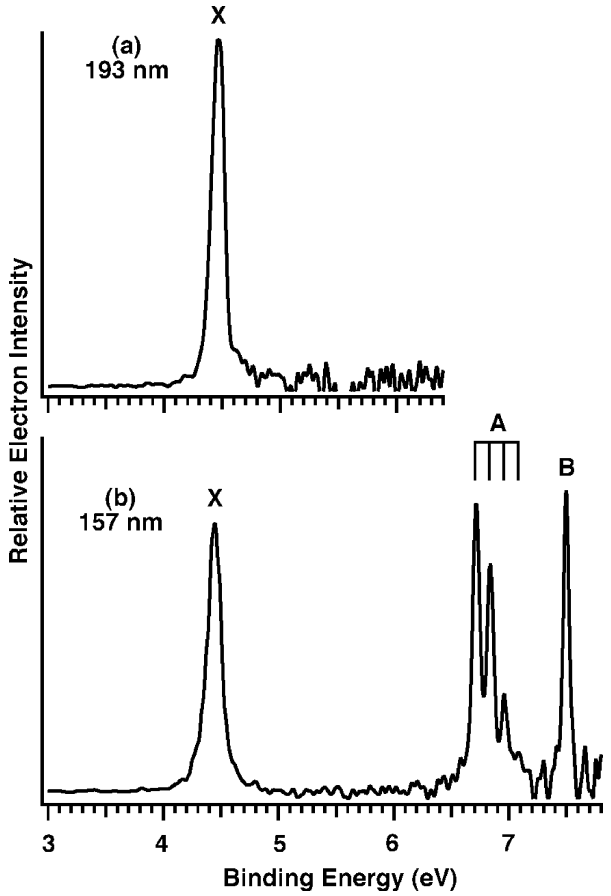

Figure 2. Photoelectron spectra of BO_2^- at (a) 193 and (b) 157 nm (7.866 eV).

4.2. BO_2^-. At the B3LYP level, both BO_2 ($^2\Pi_g$) and BO_2^- ($^1\Sigma_g^+$) possess linear geometries ($D_{\infty h}$) in their ground states. The B−O bond length is 1.262 Å in BO_2 and 1.264 Å in BO_2^-. Note that there is virtually no bond length change between the anion and the neutral, consistent with the PES spectra, which showed one vibronic peak with no vibrational progression for the ground state transition (Figure 2). The calculated ADE and VDE for BO_2^- are the same at 4.321 eV, also in agreement with the fact that there is virtually no geometry change between the ground states of BO_2^- and BO_2. The ADE and VDE calculated at the CCSD(T) level are 4.465 and 4.466 eV, respectively, slightly higher than the DFT value. The VDE's to the first and second excited states of BO_2 were calculated via TD-B3LYP to be 6.724 and 7.419 eV, respectively (Table 2).

5. Interpretation of the Photoelectron Spectra and Comparison with Theory

5.1. BO^-. *The $^2\Sigma^+$ Ground State.* The BO^- anion is a closed-shell molecule ($^1\Sigma^+$) with a valence electronic configuration of $(1\sigma)^2(2\sigma)^2(1\pi)^4(3\sigma)^2$. The corresponding molecular orbital (MO) pictures are shown in Figure 3a. Detachment of one electron from the HOMO (3σ) of the BO^- anion produces the $^2\Sigma^+$ ground state of neutral BO, yielding the first PES band (X in Figure 1). The calculated ADE and VDE, in particular at the CCSD(T) level (ADE: 2.484 eV; VDE: 2.497 eV), are in good agreement with the experimental data of 2.510 ± 0.015 eV. The current experimental EA for ^{10}BO (2.510 ± 0.015 eV) is also in excellent agreement with the previous measurement of ^{11}BO (2.508 ± 0.008 eV).[14] The isotopic shift for the EA is expected to be smaller than the experimental uncertainties in either experiment.

The HOMO (3σ) of BO^- is basically a B 2s lone pair with slight BO antibonding character (Figure 3a), consistent with the relatively short vibrational progression in the PES spectra and slight reduction in the bond length (∼0.03 Å at B3LYP level) between the anion and neutral ground states. However, the slight antibonding character of the 3σ HOMO is reflected more dramatically in the observed vibrational frequencies: 1725 cm^{-1} for $^{10}BO^-$ vs 1935 cm^{-1} for ^{10}BO. Our measured vibrational frequency for ^{10}BO agrees well with that obtained from an earlier emission spectroscopic study for ^{10}BO (1940 cm^{-1}).[4] Our observed frequencies for $^{10}BO^-/^{10}BO$ are also in line with those of $^{11}BO^-/^{11}BO$ (1665/1875 cm^{-1}) observed in the previous PES study on $^{11}BO^-$,[14] and the expected $^{10}BO/^{11}BO$ isotopic ratio of ∼1.03 is well reproduced.

The $^2\Pi$ Excited State. Removing an electron from the degenerate HOMO-1 (1π) of BO^- generates the first excited state ($^2\Pi$) of the BO neutral, which should correspond to the observed band A (Figure 1c). Note that there is a spin−orbit splitting (122 cm^{-1}) in the $^2\Pi$ state,[2] but it is too small to be resolved under our experimental conditions though it should contribute to the line widths of the vibrational features in the A band. The calculated VDE at the TD-B3LYP level is 5.900 eV for this transition, in reasonable agreement with the experimental value of 5.63 eV. The excitation energy for the $^2\Pi$ state (2.96 eV) from our PES spectrum is in excellent agreement with previous absorption spectroscopic studies.[2−5] As shown in Figure 3a, the degenerate HOMO-1 of BO^- is a strongly bonding π orbital, consistent with the broad vibrational progression of band A, which indicates a large geometry change. Furthermore, the observed ^{10}BO vibrational frequency of 1320 cm^{-1} for the $^2\Pi$ state is also much reduced in comparison to that of the $^{10}BO^-$ anion (1725 cm^{-1}), again suggesting a significant weakening of the B−O bond upon electron detach-

TABLE 2: Calculated Adiabatic and Vertical Detachment Energies (eV) for BO^- and BO_2^- Anions and Ground State Vibrational Frequencies (cm^{-1}) for BO^- and BO_2^- and Their Neutrals

			TD-B3LYP		CCSD(T)		vib freq (cm^{-1})[a]	
species	MO	final state	ADE	VDE	ADE	VDE	neutral	anion
BO^-	HOMO (3σ)	$^2\Sigma^+$	2.588	2.627	2.484	2.497	1913	1739
	HOMO-1 ($1\pi_u$)	$^2\Pi$		5.900				
BO_2^-	HOMO ($1\pi_g$)	$^2\Pi_g$	4.321	4.321	4.465	4.466	1088	1096
	HOMO-1 ($1\pi_u$)	$^2\Pi_u$		6.724				
	HOMO-2 ($2\sigma_u$)	$^2\Sigma_u^+$		7.419				

[a] The vibrational frequencies are calculated for the ^{10}B isotopic species.

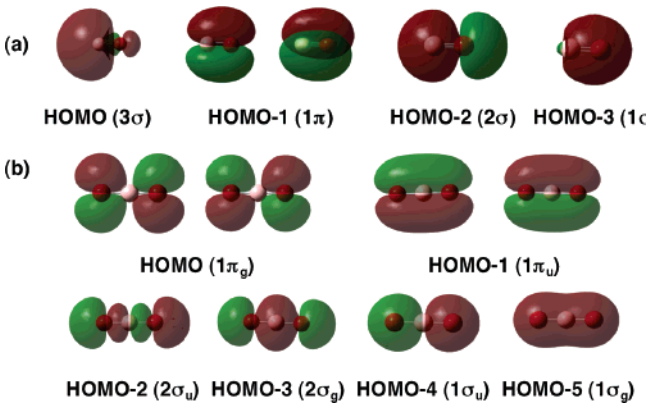

Figure 3. Valence orbital pictures of (a) BO^- and (b) BO_2^-.

ment from the 1π orbital. Our observed frequency for the $^2\Pi$ state of ^{10}BO is also in good agreement with a previous emission spectroscopic measurement (1297 cm^{-1}).[4]

Franck−Condon Factor Simulations. The well-resolved vibrational progressions and hot band transitions for the X $^2\Sigma^+$ and A $^2\Pi$ bands in the PES spectra of $^{10}BO^-$ (Figure 1) afforded us the opportunities to perform Franck−Condon factor (FCF) simulations,[33] which could yield more accurate spectroscopic constants for the ground and excited states of ^{10}BO and allow us to estimate the vibrational temperature of $^{10}BO^-$. Figure 4 displays the simulated spectra (solid curves), using a Morse oscillator,[33] compared to the experimental data (solid dots). The parameters used for the simulations are given in the figure caption. From the FCF simulations, we found a slight bond length contraction of 0.031 Å from the anion to the neutral ground state, in excellent agreement with the B3LYP results, which gives a 0.031 Å bond length change. The $^2\Pi$ excited state was found to exhibit a large bond length expansion of 0.107 Å relative to the anion. More significantly, the FCF simulation yielded a rather high vibrational temperature (1800 K) for the $^{10}BO^-$ anions, which is consistent with our prior experience that very light anions are not cooled very efficiently in our source.[33b]

5.2. BO_2^-. BO_2^- is again a closed-shell species. Our calculations show that it possesses a linear ground state ($^1\Sigma_g^+$) with a valence electron configuration of $(1\sigma_g)^2(1\sigma_u)^2(2\sigma_g)^2(2\sigma_u)^2(1\pi_u)^4(1\pi_g)^4$, in agreement with previous calculations.[8,13,20] The MO pictures are shown in Figure 3b. The HOMO is a degenerate π_g orbital, which is basically nonbonding O 2p lone pairs. Detachment from the HOMO results in the $^2\Pi_g$ ground state of BO_2. The spin−orbit splitting of the $^2\Pi_g$ state (~150 cm^{-1})[3,11i] is nearly identical with that in the isoelectronic CO_2^+,[34] but it is too small to be resolved under our experimental conditions. The calculated ADE and VDE are virtually identical (Table 2), which is in agreement with the experimental data (Table 1) and consistent with the nonbonding character of the HOMO. The CCSD(T) results (ADE: 4.465 eV; VDE: 4.466 eV) are in perfect agreement with the experimental data (ADE = VDE = 4.46 eV). The $^2\Pi_g$ ground state of BO_2 is Renner−Teller unstable along the bending coordinate.[9] However, both the sharp PES peak for the ground state transition and the theoretical calculations suggest that the Renner−Teller effect is negligible and the ground state of BO_2 remains essentially a linear molecule.[8,13,20]

Similarly, the detachment of one electron from HOMO-1 ($1\pi_u$) and HOMO-2 ($1\sigma_u$) will produce the first ($^2\Pi_u$) and second ($^2\Sigma_u^+$) excited states of BO_2, respectively. The $^2\Pi_u$ state is expected to have a spin−orbit splitting as small as the corresponding state in CO_2^+ (96 cm^{-1}),[34] which could not be resolved in our experiment. The calculated VDE's at TD-B3LYP for the transitions to the two excited states are 6.724 and 7.419 eV, respectively, which are in excellent agreement with the experimental data (6.72 and 7.50 eV). The current PES

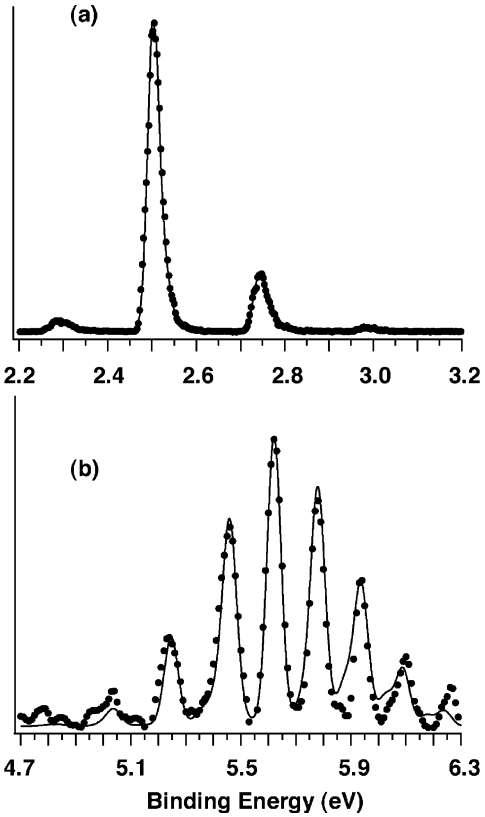

Figure 4. Franck−Condon factor simulations for the two vibrationally resolved PES bands of BO^-: (a) X ($^2\Sigma^+$) band and (b) A ($^2\Pi$) band. The dotted curves are the experimental spectra. The solid curves are the spectra simulated by fitting the calculated Franck−Condon factors with a Guassian function, 0.03 eV line width for (a) and 0.06 eV for (b). Parameters used for the simulations are the following: (a) anion frequency 1725 cm^{-1}, anharmonicity 11.5 cm^{-1}, bond length 1.236 Å; neutral frequency 1935 cm^{-1}, anharmonicity 11.5 cm^{-1}, bond length 1.205 Å; anion vibrational temperature 1800 K; (b) anion frequency 1725 cm^{-1}, anharmonicity 11.5 cm^{-1}, bond length 1.236 Å; neutral frequency 1320 cm^{-1}, anharmonicity 11.5 cm^{-1}, bond length 1.343 Å; anion vibrational temperature 1800 K.

measurements of the excitation energies for BO_2 are also in excellent agreement with the previous absorption spectroscopic study.[3]

The degenerate HOMO-1 is a strong O−B−O π-bonding orbital. Detachment from the HOMO-1 is expected to significantly weaken the B−O bond, consistent with the vibrational progression observed for the A band (Figure 2b). The observed vibrational frequency for band A of $^{10}BO_2$ (980 cm^{-1}) is indeed lower than those predicted for the ground states of BO_2 (1088 cm^{-1}) and BO_2^- (1096 cm^{-1}) (Table 2). A previous UV study reported a symmetric stretching frequency (994 cm^{-1}) for the $^2\Pi_u$ excited state of BO_2.[3] In contrast, HOMO-2 ($2\sigma_u$) is primarily an O 2p lone pair with slight B−O σ bonding character. There might be a weak vibrational progression for the B band, but our signal-to-noise ratio was too poor in the high binding energy side to allow us to make a definitive assignment.

6. Chemical Bonding in BO^- and BO_2^-

6.1. Molecular Orbital Analyses. *BO^-*. The HOMO-3 of BO^- (Figure 3a) is a σ MO primarily composed of the O 2s atomic orbital (AO), which may be roughly viewed as an O 2s lone pair. The HOMO-2 is a σ bonding MO composed of O 2p and B 2s AO's, which involves significant charge back-donation from O to B and therefore it is of strong ionic character. The degenerate HOMO-1 is a complete π bonding MO involving B and O 2p AO's. Finally, the HOMO is primarily composed of B 2s AO with slight antibonding character between B 2s and O 2p AO's, whose weak antibonding character is expected to partially cancel the bonding character in HOMO-2. The same bonding pattern holds for the BO neutral except that only one electron is filled in its HOMO. Thus, the bonding in BO and BO^- can be viewed approximately as a triple bond between B and O. The neutral BO molecule is a radical and has a slightly stronger bond than that in the anion due to the slight antibonding nature in the HOMO, which is also evidenced from the reduced Wiberg bond order: $WBI_{B=O} = 1.79$ in BO and $WBI_{B=O} = 1.57$ in BO^-.

BO_2^-. The HOMO-5 and HOMO-4 are O 2s derived bonding and antibonding orbitals (Figure 3b), which cancel each other and can be viewed as O 2s lone pairs. On the other hand, the degenerate HOMO orbitals are O 2p lone pairs, which is supported by the identical bond orders calculated for the neutral (1.58) and the anion (1.60) and consistent with the PES observation of the sharp ground state transition (Figure 2). Therefore, the OBO bonding in BO_2^- is due to HOMO-1 through HOMO-3. The HOMO-1 is a complete OBO π bonding orbital. The HOMO-2 and HOMO-3 are O 2p derived orbitals that are responsible for BO σ bonding. Overall, the bonding in BO_2^- and BO_2 can be described as two B═O double bonds.

6.2. Comparison with the Isoelectronic AlO^- and AlO_2^- Species. It is interesting to compare the current PES data with those of the isoelectronic AlO^- and AlO_2^- species.[35] The B and Al atoms are in the same group and possess almost identical s−p excitation energies (~3.6 eV) and similarly low EA's (0.28 eV for B vs 0.43 eV for Al).[36] The EA's of BO_n and AlO_n ($n = 0-2$) are compared in Figure 5. Quantitatively, the corresponding EA values are similar for the two systems within ~0.2 eV. Both EA curves show monotonic increase with oxygen content. The EA's of BO_2 (4.46 eV) and AlO_2 (4.23 eV) far exceed that of the highest atomic EA value in the periodic table (Cl: 3.61 eV, shown in Figure 5) and both BO_2 and AlO_2 belong to the class of high EA species called "superhalogens".[37] Interestingly, the EA of BO_2 is ~0.2 eV higher than that of AlO_2, despite the fact that the EA's of B and BO are both ~0.1 eV lower than those of Al and AlO (Figure 5).

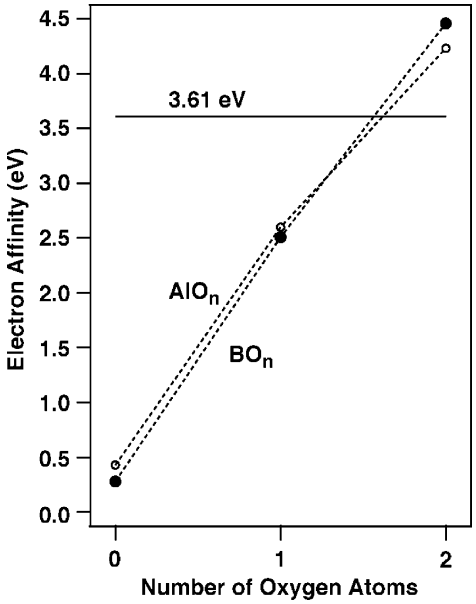

Figure 5. Comparison of electron affinities of BO_n and AlO_n ($n = 0-2$). Numbers for the B and Al atoms are from ref 36 and those for AlO and AlO_2 are from ref 35. The line drawn at 3.61 eV indicates the electron affinity of Cl, the highest known for an atom. Note that the electron affinities of both BO_2 and AlO_2 exceed that of Cl.

The ground state electron configurations for the two systems are also identical, resulting in similar overall PES patterns. However, their excitation energies are significantly different: 2.96 eV for BO vs 0.66 eV for AlO for the first excited state; 2.26 and 3.04 eV for BO_2 vs 0.65 and 0.85 eV for AlO_2 for their first and second excited states, respectively.[35] While B−O bonding is more covalent, Al−O bonding is primarily ionic. The much stronger bonding and shorter bond distance in BO (806 kJ/mol, ~1.2 Å)[38] compared to those in AlO (512 kJ/mol, ~1.6 Å)[38] make the electronic states in BO_n well separated relative to those in AlO_n. The HOMO's of all species involve little M−O (M = B, Al) interaction and show similar electron binding energies, whereas HOMO-1 and HOMO-2 reflect strong M−O bonding interactions and are sensitive to the nature of M−O interactions (B−O vs Al−O), leading to the very different excitation energies in the two systems.

6.3. Comparison with Isoelectronic Molecules CO, N_2, CN^-, and CO_2. The PES spectra of BO^- discussed above also share the same overall patterns as those of the isoelectronic species CN^-, CO, and N_2.[39] The latter three species, however, possess much higher ground state electron binding energies: 3.86 eV for CN^-,[40] 14.99 eV for CO,[39] and 15.60 eV for N_2.[39] The overall PES pattern of BO_2^- is also similar to that of the isoelectronic CO_2, which has an ionization potential of 13.78 eV.[34] The similar electronic structure of BO^- compared to CN^- and CO suggests possibilities for some interesting chemistry for BO and BO^-. Indeed, CN^- and CO are important inorganic ligands and possess rich chemistries,[21] whereas very little is known about BO and BO^- as inorganic ligands. In terms of bond strength (CO: 1076 kJ/mol; N_2: 946 kJ/mol; BO: 806 kJ/mol; CN: 770 kJ/mol; and AlO: 512 kJ/mol),[38] BO is comparable to and actually stronger than CN, and it is significantly stronger than AlO. The bond strength suggests that BO and BO^- should be rather robust chemical species and may be able to retain their integrity in chemical complexes. In addition, BO as a σ radical may either gain an extra electron to

form closed-shell BO^- analogous to CN^-, or share or lose its unpaired electron. In a recent study on $Au_n(BO)^-$ ($n = 1-3$) clusters, we indeed found that BO can maintain its chemical integrity and behaves like a monovalent unit in its bonding to Au.[26] Recent DFT theoretical studies also showed that carbon boronyls $(CBO)_n$ ($n = 3-7$) are stable molecular species.[41] Thus, it is conceivable that BO^- may indeed possess similar chemistry as CN^- or CO.

7. Conclusions

In conclusion, we report vibrationally resolved photoelectron spectroscopy of two simple boron oxide anions, $^{10}BO^-$ and $^{10}BO_2^-$, at several photon energies (355, 266, 193, and 157 nm). The electron affinities of ^{10}BO and $^{10}BO_2$ were determined to be 2.510 ± 0.015 and 4.46 ± 0.03 eV, respectively. One excited state was observed for ^{10}BO and two excited states were observed for $^{10}BO_2$. The obtained vibrational frequencies and excitation energies are consistent with previous high-resolution spectroscopic data for the neutral species. Theoretical calculations were performed at B3LYP and CCSD(T) levels for both $^{10}BO^-$ and $^{10}BO_2^-$ and their neutrals. Good agreement is observed between experiment and theory. The current PES data are also compared with those of the isoelectronic AlO^- and AlO_2^- species and the closely related molecules CO, N_2, CN^-, and CO_2, suggesting possibilities for BO and BO^- as potential new inorganic ligands.

Acknowledgment. We thank Dr. Jun Li for invaluable discussions and help with the theoretical calculations. This work was supported by the National Science Foundation (DMR-0503383) and was performed at the W. R. Wiley Environmental Molecular Sciences Laboratory, a national scientific user facility sponsored by DOE's Office of Biological and Environmental Research and located at the Pacific Northwest National Laboratory, operated for DOE by Battelle. S.D.L. gratefully acknowledges the financial support from the Natural Science Foundation of China (No. 20573088) and the hospitality and support of the Summer Institute of Chemical Physics at Pacific Northwest National Laboratory during this work.

References and Notes

(1) Bauer, S. H. *Chem. Rev.* **1996**, *96*, 1907.
(2) Huber, K. P.; Herzberg, G. *Constants of Diatomic Molecules*; Van Nostrand Reinhold: New York, 1979.
(3) Johns, J. W. C. *Can. J. Phys.* **1961**, *39*, 1738.
(4) Melen, F.; Dubois, I.; Bredohl, H. *J. Phys. B*: *At. Mol. Phys.* **1985**, *18*, 2423.
(5) (a) Melen, F.; Dubois, I.; Bredohl, H. *J. Mol. Spectrosc.* **2001**, *208*, 14. (b) Osiac, M.; Ropcke, J.; Davies, P. B. *Chem. Phys. Lett.* **2001**, *344*, 92. (c) Stancu, G. D.; Ropcke, J.; Davies, P. B. *J. Mol. Spectrosc.* **2004**, *223*, 181.
(6) (a) Clyne, M. A. A.; Heaven, M. C. *Chem. Phys.* **1980**, *51*, 299. (b) Burkholder, T. R.; Andrews, L. *J. Chem. Phys.* **1991**, *95*, 8697.
(7) (a) Griffing, K. M.; Simons, J. *J. Chem. Phys.* **1976**, *64*, 3610. (b) Peterson, K. A.; Woods, R. C. *J. Chem. Phys.* **1989**, *90*, 7239. (c) Ziegler, T.; Gutsev, G. L. *J. Comput. Chem.* **1992**, *13*, 70. (d) Yeager, D. L.; Nichols, J. A.; Golab, J. T. *J. Chem. Phys.* **1992**, *97*, 8441.
(8) Mota, F.; Novoa, J. J.; Ramirez, A. C. *J. Mol. Struct.* (*Theochem*) **1988**, *166*, 153.
(9) Herzberg, G. *Electronic Spectra of Polyatomic Molecules*; Van Nostrand Reinhold: New York, 1976.
(10) Sommer, A.; White, D.; Linevsky, M. J.; Mann, D. E. *J. Chem. Phys.* **1963**, *38*, 87.
(11) (a) Russell, D. K.; Kroll, M.; Dows, D. A.; Beaudet, R. A. *Chem. Phys. Lett.* **1973**, *20*, 153. (b) Dixon, R. N.; Field, D.; Noble, M. *Chem. Phys. Lett.* **1977**, *50*, 1. (c) Fried, A.; Mathews, C. W. *Chem. Phys. Lett.* **1977**, *52*, 363. (d) Lowe, R. S.; Gerhardt, H.; Dillenschneider, W.; Curl, R. F.; Tittel, F. K. *J. Chem. Phys.* **1979**, *70*, 42. (e) Weyer, K. G.; Beaudet, R. A.; Straubinger, R.; Walther, H. *Chem. Phys.* **1980**, *47*, 171. (f) Kawaguchi, K.; Hirota, E. *J. Mol. Spectrosc.* **1986**, *116*, 450. (g) Maki, A. G.; Burkholder, J. B.; Sinha, A.; Howard, C. J. *J. Mol. Spectrosc.* **1988**, *130*, 238. (h) Chow, J. R.; Beaudet, R. A.; Schulz, W.; Weyer, K.; Walther, H. *Chem. Phys.* **1990**, *140*, 307. (i) Agreiter, J.; Lorenz, M.; Smith, A. M.; Bondybey, V. E. *Chem. Phys.* **1997**, *224*, 301.
(12) (a) Saraswathy, V.; Diamond, J. J.; Segal, G. A. *J. Phys. Chem.* **1983**, *87*, 718. (b) Csaszar, P.; Kosmus, W.; Panchenko, Y. N. *Chem. Phys. Lett.* **1986**, *129*, 282.
(13) Ortiz, J. V. *J. Chem. Phys.* **1993**, *99*, 6727.
(14) Wenthold, P. G.; Kim, J. B.; Jonas, K. L.; Lineberger, W. C. *J. Phys. Chem. A* **1997**, *101*, 4472.
(15) Srivastava, R. D.; Uy, O. M.; Farber, M. *Trans. Faraday. Soc.* **1971**, *67*, 2941.
(16) Jensen, D. E. *J. Chem. Phys.* **1970**, *52*, 3305.
(17) Rienstra, J. C.; Schaefer, H. F. *J. Chem. Phys.* **1997**, *106*, 8278.
(18) (a) Ortiz, J. V. *Chem. Phys. Lett.* **1998**, *296*, 494. (b) Jursic, B. S. *J. Mol. Struct.* (*Theochem*) **1999**, *467*, 1. (c) Papakondylis, A.; Mavridis, A. *Chem. Phys. Lett.* **2001**, *341*, 382. (d) Stampfuss, P.; Wenzel, W. *Chem. Phys. Lett.* **2003**, *370*, 478.
(19) Jensen, D. E. *Trans. Faraday Soc.* **1969**, *65*, 2123.
(20) Zakrzewski, V. G.; Boldyrev, A. I. *J. Chem. Phys.* **1990**, *93*, 657.
(21) Cotton, F. A.; Wilkinson, G.; Murillo, C. A.; Bochmann, M. *Advanced Inorganic Chemistry*, 6th ed.; John Wiley & Sons: New York, 1999.
(22) (a) Zhai, H. J.; Wang, L. S.; Alexandrova, A. N.; Boldyrev, A. I. *J. Chem. Phys.* **2002**, *117*, 7917. (b) Alexandrova, A. N.; Boldyrev, A. I.; Zhai, H. J.; Wang, L. S.; Steiner, E.; Fowler, P. W. *J. Phys. Chem. A* **2003**, *107*, 1359. (c) Zhai, H. J.; Wang, L. S.; Alexandrova, A. N.; Boldyrev, A. I.; Zakrzewski, V. G. *J. Phys. Chem. A* **2003**, *107*, 9319. (d) Alexandrova, A. N.; Boldyrev, A. I.; Zhai, H. J.; Wang, L. S. *J. Phys. Chem. A* **2004**, *108*, 3509. (e) Zhai, H. J.; Alexandrova, A. N.; Birch, K. A.; Boldyrev, A. I.; Wang, L. S. *Angew. Chem., Int. Ed.* **2003**, *42*, 6004. (f) Zhai, H. J.; Kiran, B.; Li, J.; Wang, L. S. *Nat. Mater.* **2003**, *2*, 827. (g) Kiran, B.; Bulusu, S.; Zhai, H. J.; Yoo, S.; Zeng, X. C.; Wang, L. S. *Proc. Natl. Acad. Sci. U.S.A.* **2005**, *102*, 961.
(23) Alexandrova, A. N.; Boldyrev, A. I.; Zhai, H. J.; Wang, L. S. *Coord. Chem. Rev.* **2006**, *250*, 2811.
(24) (a) Alexandrova, A. N.; Zhai, H. J.; Wang, L. S.; Boldyrev, A. I. *Inorg. Chem.* **2004**, *43*, 3552. (b) Alexandrova, A. N.; Boldyrev, A. I.; Zhai, H. J.; Wang, L. S. *J. Chem. Phys.* **2005**, *122*, 054313.
(25) (a) Zhai, H. J.; Wang, L. S.; Zubarev, D. Yu.; Boldyrev, A. I. *J. Phys. Chem. A* **2006**, *110*, 1689. (b) Zubarev, D. Yu.; Li, J.; Wang, L. S.; Boldyrev, A. I. *Inorg. Chem.* **2006**, *45*, 5269.
(26) Zubarev, D. Yu.; Boldyrev, A. I.; Li, J.; Zhai, H. J.; Wang, L. S. *J. Phys. Chem. A.* Submitted for publication.
(27) (a) Wang, L. S.; Cheng, H. S.; Fan, J. *J. Chem. Phys.* **1995**, *102*, 9480. (b) Wang, L. S.; Wu, H. In *Advances in Metal and Semiconductor Clusters. IV. Cluster Materials*; Duncan, M. A., Ed.; JAI: Greenwich, CT, 1998; pp 299−343.
(28) (a) Becke, A. D. *J. Chem. Phys.* **1993**, *98*, 5648. (b) Lee, C.; Yang, W.; Parr, R. G. *Phys. Rev. B* **1988**, *37*, 785.
(29) Kendall, R. A.; Dunning, T. H.; Harrison, R. J. *J. Chem. Phys.* **1992**, *96*, 6796.
(30) Frisch, M. J.; Trucks, G. W.; Schlegel, H. B.; et al. *Gaussian 03*; Gaussian, Inc.: Pittsburgh, PA, 2003.
(31) (a) Casida, M. E.; Jamorski, C.; Casida, K. C.; Salahub, D. R. *J. Chem. Phys.* **1998**, *108*, 4439. (b) Bauernschmitt, R.; Ahlrichs, R. *Chem. Phys. Lett.* **1996**, *256*, 454.
(32) (a) Cizek, J. *Adv. Chem. Phys.* **1969**, *14*, 35. (b) Scuseria, G. E.; Schaefer, H. F. *J. Chem. Phys.* **1989**, *90*, 3700.
(33) (a) Wang, L. S.; Niu, B.; Lee, Y. T.; Shirley, D. A.; Balasubramanian, K. *J. Chem. Phys.* **1990**, *92*, 899. (b) Kim, J. H.; Li, X.; Wang, L. S.; de Clercq, H. L.; Fancher, C. A.; Thomas, O. C.; Bowen, K. H. *J. Phys. Chem. A* **2001**, *105*, 5709. (c) Zhai, H. J.; Kiran, B.; Wang, L. S. *J. Phys. Chem. A* **2003**, *107*, 2821.
(34) Wang, L. S.; Reutt, J. E.; Lee, Y. T.; Shirley, D. A. *J. Electron Spectrosc. Relat. Phenom.* **1988**, *47*, 167.
(35) (a) Desai, S. R.; Wu, H.; Wang, L. S. *Int. J. Mass Spectrom. Ion Processes* **1996**, *159*, 75. (b) Desai, S. R.; Wu, H.; Rohlfing, C. M.; Wang, L. S. *J. Chem. Phys.* **1997**, *106*, 1309.
(36) Rienstra-Kiracofe, J. C.; Tschumper, G. S.; Schaefer, H. F.; Nandi, S.; Ellison, G. B. *Chem. Rev.* **2002**, *102*, 231.
(37) Gutsev, G. L.; Boldyrev, A. I. *Adv. Chem. Phys.* **1985**, *61*, 169.
(38) Dean, J. A. *Lange's Handbook of Chemistry*, 15th ed.; McGraw-Hill: New York, 1999.
(39) Kimura, K.; Katsumata, S.; Achiba, Y.; Yamazaki, T.; Iwata, S. *Handbook of He I Photoelectron Spectra of Fundamental Organic Molecules*; Japan Scientific Societies Press: Tokyo, Japan, 1981.
(40) Bradforth, S. E.; Kim, E. H.; Arnold, D. W.; Neumark, D. M. *J. Chem. Phys.* **1993**, *98*, 800.
(41) (a) Li, S. D.; Miao, C. Q.; Guo, J. C.; Ren, G. M. *J. Comput. Chem.* **2005**, *26*, 799. (b) Ren, G. M.; Li, S. D.; Miao, C. Q. *J. Mol. Struct.* (*Theochem*) **2006**, *770*, 193.